

## IAC-08-C1.6.2

### FORMATION FLYING OF A TELESCOPE/OCCULTER SYSTEM WITH LARGE SEPARATIONS IN AN L2 LIBRATION ORBIT

Mr. David Folta  
NASA Goddard Space Flight Center,  
Greenbelt, MD, 20771, USA  
[david.c.folta@nasa.gov](mailto:david.c.folta@nasa.gov)

Mr. Jonathan Lowe  
Analytical Graphics Inc.  
Exton, PA 19341, USA  
[jlowe@agi.com](mailto:jlowe@agi.com)

#### ABSTRACT

Flying an occulter in formation with a telescope in a sun-Earth L2 co-linear libration orbit requires an understanding of the interactions between the dynamics and limitations of the three-body restricted system and formation control methods. When the formation separation distances become a large fraction of the telescope's libration orbit amplitude, linear approximations break down and formation control becomes problematic, requiring high-fidelity modeling and specific targeting methods. This paper considers control approaches and determines  $\Delta V$  requirements to re-align the New Worlds Observer telescope-occulter formation and to maintain the viewing geometry during an observation sequence. Analyzed for both impulsive and finite (low-thrust) maneuvers using two different Lissajous classes, a feasible mission design is found with control cost ( $\Delta V$ ) in the km/sec range.

#### INTRODUCTION

Flying an occulter in formation with a telescope in a sun-Earth L2 co-linear libration orbit requires an understanding of the interactions between the dynamics of the three-body restricted system and formation control methods. When the separation distances between the two spacecraft become a large fraction of the telescope's libration orbit amplitude and the occulter follows an unnatural libration orbit, linear approximations break down and formation control becomes problematic, requiring high-fidelity modeling and specific targeting methods.

Recently NASA's Goddard Space Flight Center (GSFC) began a study of such a system of spacecraft for the New Worlds Observer (NWO) mission. The study investigates control methods and determines

mission implementation control cost ( $\Delta v$  and fuel mass). Further complicating the system control is the requirement to achieve deterministic occulter positions relative to the telescope in a timed sequence for science observations. These target positions align the system to observe selected star/planet systems as they become visible in the field of regard. The occulter is constrained to a large separation distance from the telescope that approaches 30% of its libration orbit x-axis amplitude, yielding uncharacteristic motion instead of the usual natural Lissajous orbit.

This paper considers the use of differential correction (DC) vice linear control techniques for control approaches. The  $\Delta V$  requirements to re-align the telescope-occulter system and the  $\Delta V$  to maintain the viewing geometry during an observation sequence are determined. Control costs ( $\Delta V$

## IAC-08-C1.6.2

and fuel mass) are derived from DC targeting using impulsive (chemical) and finite (low-thrust) maneuvers implemented in a full-ephemeris model with numerical (Runga-Kutta) integration. The impulsive approach implements a traditional two-maneuver boundary value concept with the boundary conditions determined only by position and time constraints. The finite maneuver implementation uses a constant low-thrust maneuver with combinations of boundary conditions derived from position, velocity, and time. The DC process is used in both impulsive and finite maneuver applications and is compared to an optimization process to determine possible improvements or inconsistencies. Total mission  $\Delta V$  cost and the influence of various observation sequences are presented, and an approach to permit extended separation formations is addressed.

### The New Worlds Observer Mission

The New Worlds Observer (NWO) mission is a next step in the search for new worlds that may harbor life throughout the galaxy. NWO will be able to identify planetary features like oceans, continents, polar caps and cloud banks and even detect biomarkers like methane, oxygen and water if they exist. "NWO will study Earth-like planets tens of trillions of miles away and chemically analyze their atmospheres for signs of life."<sup>1,2,3</sup> Figures 1 and 2 show diagrams of the NWO system.



Figure 1: View Of NWO Telescope and Occulter Pointed at Star/Planetary System (credit Northrop Grumman Space Technology)

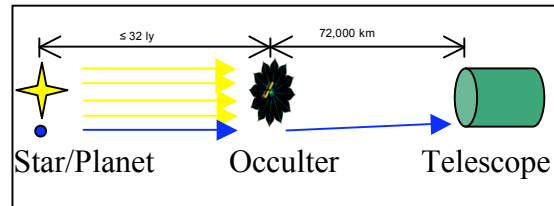


Figure 2: NWO System Design Concept

The components of NWO are a telescope and an occulter. The system works in the Fresnel regime using diffraction around an "apodized" occulter. The light destructively interferes in the center creating a zone of deep shadow with better than  $10^{-10}$  contrast suppression. The destructive interference in the optical near field is permitted by specially-shaped petals on the occulter. The system works simply by blocking the on-axis star light with the telescope looking off-axis to observe companions. The occulter is a disk approximately 40 meters in diameter. The separation distance between the telescope and the occulter is a function of the diameter of the occulter and can range (for this study) from 38,700 km to 72,000 km. The 72,000 km (38,700 km) separation corresponds to a 40 m (20 m) diameter occulter.

The orbit goals for the NWO mission require a telescope to orbit the sun-Earth L2 co-linear libration point while the occulter orbits in an unnatural, forced trajectory that allows observation of the star and companion planet over several days. During an observation, the occulter must maintain alignment with the telescope. While this alignment can be represented as a spherical accuracy, a two component accuracy best describes this goal as a radial - line of sight direction held to 100m, and a tangent to the line of sight held to a few meters. These requirements are not controlled during the transfer from the end of one observation to the start of the next observation.

### Analysis Goals

The goal of this paper is very basic: determine the impulsive  $\Delta V$  and fuel used

## IAC-08-C1.6.2

over the mission lifetime for a chemical or low-thrust system to maneuver the occulter from the end of one observation to the start of the next. For a given telescope orbit, we determine the ideal occulter position relative to the telescope for each observation with the order and schedule fixed by the star sequence used. While these  $\Delta V$ s should represent the control cost, they are not optimized. Stationkeeping was not implemented during the observation arc. The only targeted goal used was to be at the beginning and end of a given observation arc at the required time.

### NWO TRAJECTORY DESIGN

The selection of the nominal L2 collinear telescope orbit was, for this study, solely determined by its impact on occulter control cost. While the telescope orbit has not been predefined, two libration classes were investigated. The two orbits chosen are an orbit similar to that of the James Webb Space Telescope (JWST), a Class-II halo with an anticlockwise rotation (when looking at the Sun) with y-amplitude of 750,000 km, and a Class-I clockwise rotation (when looking at the sun) orbit that has a y-amplitude of 660,000 km. The Class-I was chosen as the baseline orbit for this analysis and is taken from a Northrop Grumman (NG) study.<sup>3</sup> The comparison of these orbits is shown in Figures 3 and 4.

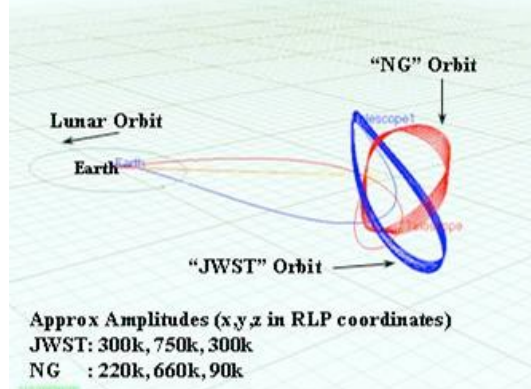


Figure 3: JWST (Blue) and Baseline (Red) Orbit Comparison

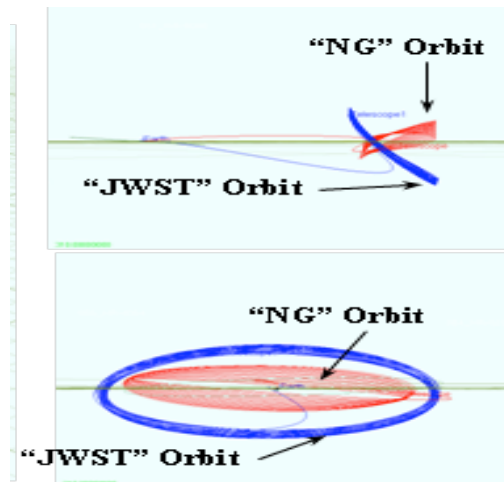


Figure 4: The JWST (Blue) and Baseline (Red) Orbits

Stationkeeping maintenance of the nominal telescope orbit was not considered as a driving requirement on the NWO system since the maintenance cost is very small in comparison to the occulter transfer cost. The analysis uses a pre-generated balanced (multiple revolution) orbit for the telescope that spans 5 years. Starting with the initial condition of the telescope, the occulter is then ‘released’ upon entering the libration orbit and flown to the first observation target location where it follows a short trajectory arc to the end of the observation. From the end point, a trajectory must be defined such that the occulter arrives at the next target location at a preset time to begin the next observation. This process is repeated until all desired targets have been observed.

### The Target Selection Process and DRM Target Sequence

The NWO science team defined a timed sequence of observation targets called the Design Reference Mission (DRM).<sup>4</sup> Five DRMs were generated based on occulter size and the selected star sequence. Figures 5 and 6 show a sample of DRM #4 and DRM #5 targets on a sphere centered at the L2 point in a rotating coordinate frame. Note that the grouping of the stars is mostly

## IAC-08-C1.6.2

perpendicular to the Earth-sun line. In order to determine the ideal location of the occulter for each observation, the vector from the telescope to the target star is constructed using the inertial right ascension and declination. The point along this vector at the required separation distance from the telescope is reported throughout the observation period, thus creating an “ideal observation ephemeris” consisting of many discontinuous arcs as shown in Figures 7 through 9.

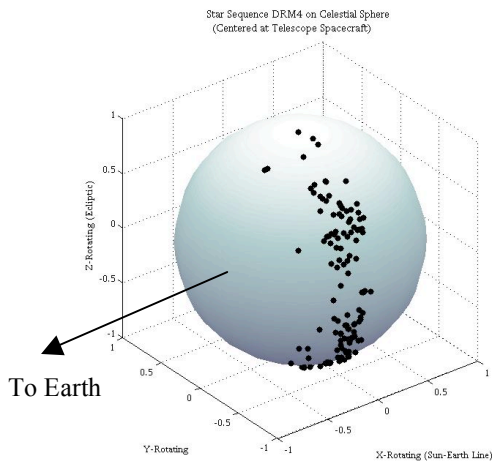


Figure 5: DRM-4 Distribution of Stars on Sphere in a Sun-Earth Rotating Coordinate System

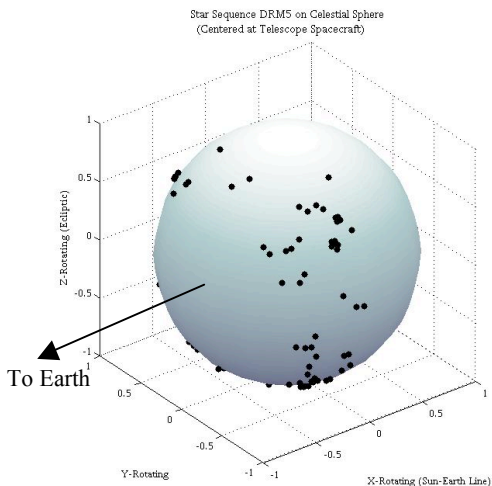


Figure 6: DRM-5 Distribution of Stars on Sphere in a Sun-Earth Rotating Coordinate System

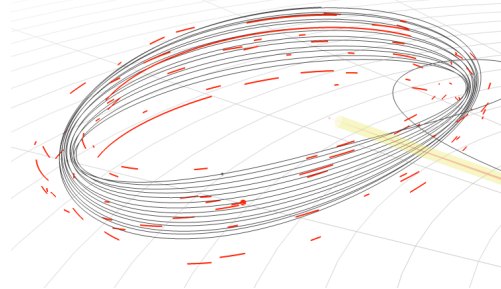


Figure 7: Oblique View of Ideal Arcs and the Reference Telescope Orbit in a Rotating System

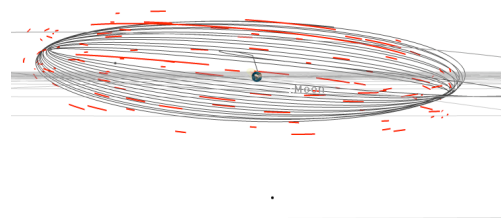


Figure 8: X-Axis View of Ideal Arcs and the Reference Telescope Orbit in a Rotating System

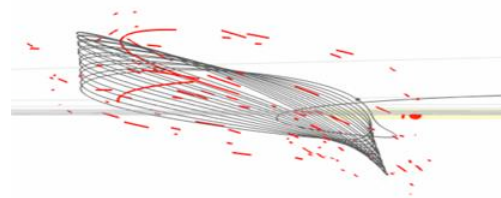


Figure 9: Y-Axis View of Ideal Arcs and the Reference Telescope Orbit in a Rotating System

Several DRM sequences were analyzed to determine the impact of the observation sequence on the total control costs of the mission. Another complexity to the target start sequence is that any given star can also be viewed multiple times at different epochs while it is in the field of regard. This revisit occurs after the occulter has been repositioned to another target.

The type of information provided in the DRM is as follows:

- 1) Hipparcos number of the star
- 2) Exposure time in days

## IAC-08-C1.6.2

- 3) Time1 - Time when occulter arrives at the target (days since Jan 1, 2015 00:00:00)
- 4) Time2 - time when the occulter leaves the target
- 5) Right Ascension of the target (degrees)
- 6) Declination of the target (degrees)
- 7) Slew Angle to get to the target from the previous target
- 8) Estimated Delta-V assuming a  $5e-5$  m/s<sup>2</sup> acceleration

### DRM Transfer Trajectory Modeling

An exploratory investigation using the conventional Circular Restricted Three-Body (CRTB) problem and linear approximations determined an initial  $\Delta V$  cost.<sup>5,6,7,8</sup> The concern with this approach is the use of a linear approximation, which assumes that the occulter is flying close to a Lissajous reference orbit during the transfer (or even during the observation trajectory) and behaving in a manner directed by the three-body dynamics. The dependency on CRTB motion and a controller with respect to a reference orbit using continuous control effort does not allow an easy operational approach. For example, analysis that depends upon the stability and the configuration and dimensions of the formation for the MAXIM mission design was completed using three-body dynamics, but only required the continuous-pointing for overall-observation arcs.<sup>9</sup> Also, control comparisons for formations that are either leader-follower or near to a libration orbit were presented by Farrar and Millard. In that analysis, the emphasis was on the utilization of natural motions in the Lagrangian regions to minimize the control efforts via Proportional – Integral – Derivative (PID), Linear Quadratic Regulator (LQR), Sliding Mode Control (SMC), or Feedback Linearization (FL). There is also the possible need to discretize the control effort for these systems as well. The use of linearization requires that the separation distances are constrained such that the controlled trajectory lies near a reference,

and the control may become asymptotic. In this analysis, we have no reference other than the ‘ideal’ occulter points, and must consider real operational impacts. The NWO separation distance of 70,000km and its requirement to achieve the target locations within a fixed time drives the states (both position and velocities) between transfer points to follow unnatural (but heliocentric-like) paths. Therefore, linear reference approaches may not be appropriate when compared to an operational setting that relies on full numerical ephemeris model with perturbations and epoch driven relative positions.

### DYNAMICS OF LIBRATION FORMATIONS

Nonetheless, for comparison, an analysis using a leader-follow concept with CRTB dynamic motion along with a comparison to analysis by Millard was made. For the leader-follower, a LQR provided the control effort. A MATLAB® Simulink setup for this analysis used a CRTB pseudo-gravitational matrix for both the reference (telescope) orbit and the occulter. The occulter held a constant offset of only 30,000 km for this case. The occulter followed a Lissajous orbit design similar to the reference, which is not the realistic motion.

In addition to the use of the pseudo-gravitational matrix, a monodromy matrix and eigenvalue information can also be generated that provides information on the stability of the system. This approach works well for the maintenance of the telescope where GSFC experience in the operations of multiple libration orbiting spacecraft such as SOHO and WMAP indicates that the control cost for the telescope is a few meters per second per year if maneuvered to counter the unstable mode. The trajectory of the occulter in its transfer between target locations may not afford one to compute a monodromy matrix since the trajectory for the ‘arc’ is not quasi-periodic. In addition, the computation of Eigen-information is of

## IAC-08-C1.6.2

limited use since the transfer trajectory is already on an unstable direction or in fact it may be heliocentric.

### Analysis Modeling and Targeting

With the decision not to apply CRTB or Monodromy information, another method needs to be chosen for accurate analysis. The commercially available software tool *STK/Astrogator*<sup>10</sup>, written by Analytical Graphics, Inc.<sup>11</sup>, has been employed by GSFC for maneuver planning and trajectory design, analysis, operations for numerous missions over the past ten years. It can compute trajectories using high fidelity, operational quality force modeling and numerical integration. Users can implement detailed control schemes using impulsive or finite maneuvers. *STK/Astrogator* also utilizes a Newton-Raphson differential corrector using singular value decomposition to solve for any input parameter, including impulsive and finite maneuvers. It is also fully integrated with *STK*, allowing users to easily analyze dynamic geometries, attitude, contact times, and more. It also allows users to fully automate and customize workflows. The DC approach used is the traditional method based on the following;

- Newton-Raphson
- Truncated Taylor series solved numerically
- Sensitivity matrix for >1 variables (x & y) and goals (A & B)
- Gauss-Jordan Elimination used for inversion
- Perturbations,  $\Delta x$  and  $\Delta y$ , are user defined
- Finite difference used to compute derivatives

The DC implementation is shown here for information, with the customary sensitivity matrix, variables, goals, and tolerances.

$$\begin{aligned}f(x + \Delta x, y + \Delta y) &= A \\g(x + \Delta x, y + \Delta y) &= B\end{aligned}$$

$$\begin{bmatrix} x_1 \\ y_1 \end{bmatrix} \approx \begin{bmatrix} x_0 \\ y_0 \end{bmatrix} + \begin{bmatrix} \frac{\partial f}{\partial x} & \frac{\partial f}{\partial y} \\ \frac{\partial g}{\partial x} & \frac{\partial g}{\partial y} \end{bmatrix}^{-1} \begin{bmatrix} A - f(x, y) \\ B - g(x, y) \end{bmatrix}$$

### Implementation of the Star data

*STK* includes a star catalog which is available for geometric and other analysis. Each of the desired targets of a particular DRM was imported from the catalog. From its orbit, the telescope spacecraft was set to point toward each of the targeted stars at the appropriate intervals. Using *STK*'s Vector Geometry Tool, a point was defined along the axis of the spacecraft at the required occulter separation distance. *STK*'s time-dynamic geometry engine then handles all coordinate frame transformations and computations in a programmatic way without requiring detailed user input. The Earth-centered J2000 location of the point was then reported for each observation interval to establish the start and end goals for each observation, as well as a complete ideal occulter ephemeris.

### The Impulsive Sequence

The targeting approach taken for the impulsive case was a simple boundary constraint on the start and end of each observation. Beginning at the same location as the telescope, the occulter would perform an impulsive maneuver which would cause it to arrive at the ideal position for the first observation at the appropriate time. The occulter spacecraft then coasts to this location. Upon arrival it performs another maneuver that will cause it to pass through the end point of the given observation arc at the appropriate time. The occulter again coasts through the observation and, on arrival at the end point, performs another maneuver that will cause it to arrive at the starting point of the next observation at the appropriate time – where the entire process is repeated. Figure 10 shows a notional diagram of this process.

## IAC-08-C1.6.2

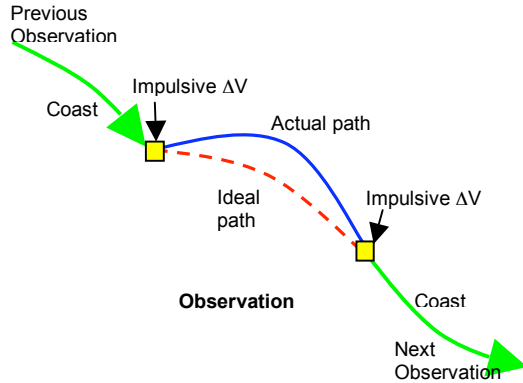


Figure 10: Notional Diagram of Impulsive Trajectory Approach

Each coasting phase of the mission was set only to propagate until the appropriate epoch, since all the times are predetermined by the DRM. The differential corrector was configured to use two profiles which run sequentially, each solving one sub-problem. The first profile varied the X, Y, and Z components of the  $\Delta V$  vector of the first maneuver such that the X, Y, and Z position of the occulter at the end of the coasting transfer phase matched the ideal X, Y, and Z position to within a 1-meter tolerance. The second profile controlled the X, Y, and Z components of the second  $\Delta V$  to make the coordinates of the occulter at the end of the observation match the ideal X, Y, and Z position to within 1 meter.

Each impulsive run resulted in a complete ephemeris for the occulter as well as a  $\Delta V$  history for the entire mission. Additionally, it defined a complete position and velocity state that the occulter must achieve at each waypoint on the trajectory in order to arrive at the next waypoint at the proper time. These state vectors were not yet optimized for any purpose. As such, the path taken by the occulter during a given observation is only within mission tolerances at the beginning and end of the arc, not throughout the duration. Finally, Astrogator reports the estimate of the finite burn duration for a selected engine to achieve the  $\Delta V$  computed from the impulsive maneuver; this estimate is based solely on the rocket equation, not

on an integrated trajectory. This process is called “seeding” a finite maneuver. For this analysis, a simple engine model with constant thrust of 0.9 N and constant Isp of 4100 s was used.

Figure 11 and 12 show the DC process in Astrogator for the first target. The starting location of the occulter is at the telescope location. The green lines indicate the transfer while the blue and red (final) show the observation arc. Figure 10 best describes the first  $\Delta V$  for the transfer while Figure 11 shows the  $\Delta V$  for the observation arc.

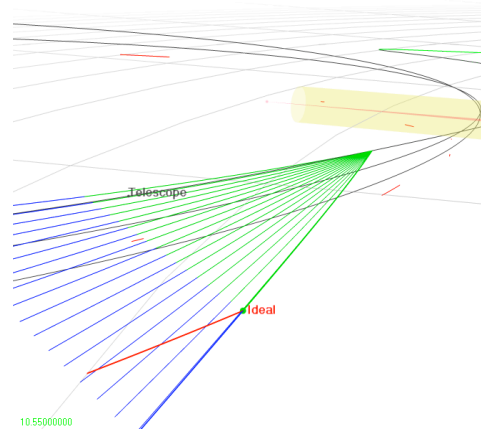


Figure 11: Impulsive Transfer Trajectory for First Star Transfer

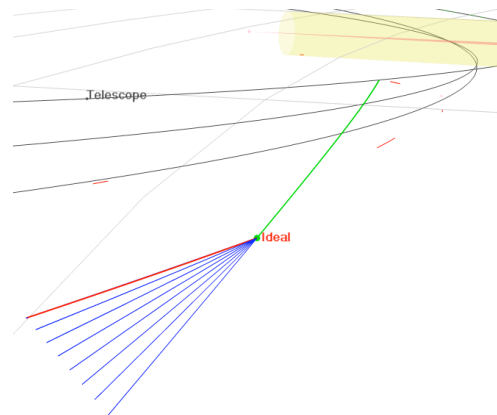


Figure 12: Impulsive Transfer Trajectory for Observation Arc

## IAC-08-C1.6.2

Figure 13 show the occulter 'orbit' for several transfer and observation arcs. Note the separation distance to the reference Lissajous orbit.

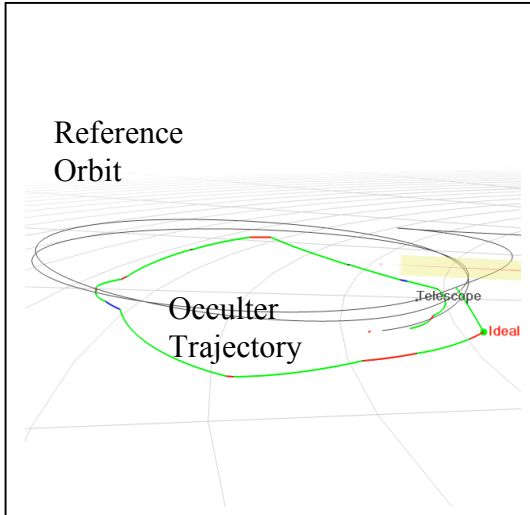


Figure 13: Impulsive Transfer Trajectory for Several Observation Arcs

### The Finite (Low-Thrust) Sequence

Utilizing low-thrust, finite maneuvers for the control sequence requires a very different setup from the impulsive case. The primary differences are that each maneuver may be days long and all thrusting must finish before reaching the observation arc. There are two finite burns separated by a coasting period during each transfer between observation arcs. The first maneuver begins at the end of one observation while the second maneuver finishes just as the next observation arc starts, as seen in Figure 12.

Each finite maneuver propagates the ephemeris until the desired duration of the maneuver has been reached. Similarly, the coast phase must be set to stop on duration instead of the next observation starting epoch. Although each of these three durations are unknown and will be solved for, good initial guesses are provided by seeding the finite maneuvers from the impulsive ones. The initial guess for the coast phase is obtained simply by subtracting the sum of the low-thrust burn

durations from the total time between observations.

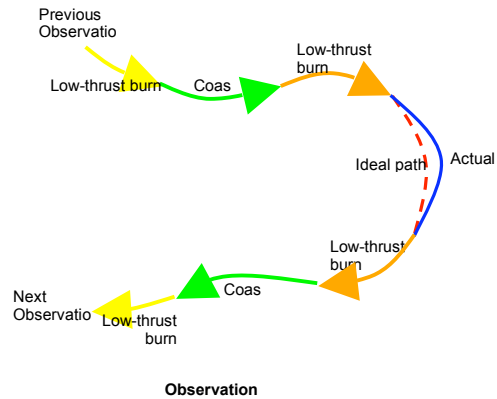


Figure 14: Diagram of Low-Thrust Trajectory Approach

The differential corrector setup required for the finite maneuver case is also quite different than for the impulsive case. The impulsive case, computed prior to running the finite case, results in a state vector (position, velocity, and epoch) for the start of the observation which will also satisfy the conditions at the end of the observation. By precisely matching this state vector, the low-thrust case need not be directly constrained to match conditions at the end of the observation arc. The two solved profiles from the impulsive case were applied to give good initial guesses for the maneuver direction and duration as well as the coast duration. Two additional profiles were then added to the differential corrector, which get incrementally closer to matching the required state vector at the start of a given observation. The first profile varies the azimuth, elevation, and duration of the first burn and the duration of the coast to achieve only the epoch, X, Y, and Z position at the start of the observation. The second profile varies the azimuth, elevation, and duration of both the first and second burns and the duration of the coast to achieve the X, Y, Z components of position and the VX, VY, and VZ components of velocity at the epoch of the start of the observation. All final solutions converged within at least 1 meter

## IAC-08-C1.6.2

in position and 10 cm/s in velocity of the desired values. Figure 13 shows the occulter transfer trajectories for several observations.

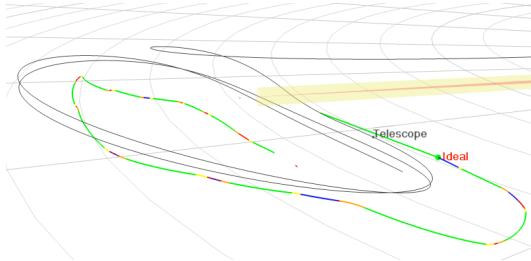


Figure 15: Finite Maneuver Transfer Trajectory for Several Observation Arcs

### Automation and Custom Workflow

Because of the complex setup required for each observation and the number of targets in each DRM considered (~100), the entire process described above was automated. The STK/Integration module offers many options for automating STK or fully integrating it into an external software system. The method chosen for this analysis was to create an HTML page embedded within STK running JavaScript. The HTML page shown in Figure 15 communicated with STK over a Microsoft COM connection and sent commands and received data via STK's Connect interface. Connect is simply a series of specially-formatted ASCII text strings which STK interprets for input and output and commanding.

An overview of the automation process follows:

1. The user inputs some initial setup information, such as the occulter separation distance, a Comma separated Value (CSV) file containing the targets and epochs of a desired DRM, and the epoch the occulter first separates from the telescope spacecraft once in an L2 orbit.

2. Selecting the "Import .csv" button parses the file, imports the targets to STK as star objects, and populates the table at the bottom of the page with the epochs of each observation arc.

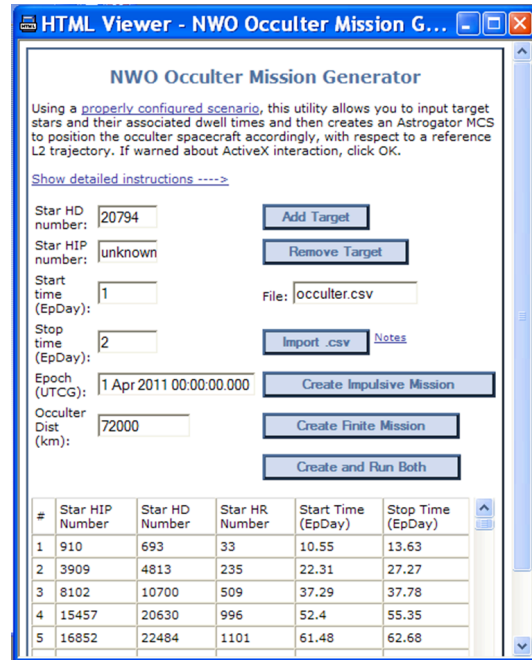


Figure 16: Automation Interface to Input DRM and Control Simulation

3. Selecting the "Create Impulsive Mission" button causes the following to take place: the ideal occulter point is constructed, an ephemeris is created from this point, and information from this ephemeris is used to construct the control sequence of maneuvers, propagations, and differential corrector profiles required for the impulsive case. Each observation arc contains position and epoch information computed for the given DRM and separation distance.

4. The user can now inspect the impulsive case setup before starting the DC and propagation of the trajectory.

5. Selecting the "Create Finite Mission" button creates a copy of the spacecraft and control sequence used in the solved impulsive case and modifies it to use appropriate stopping conditions for the low-thrust case, seed the finite maneuvers from the impulsive case, estimate coast durations, and input velocity and epoch constraints for each observation arc.

## IAC-08-C1.6.2

6. The user can now inspect the low-thrust case setup before starting the DC and propagation of the trajectory.

7. Given the run-time required to compute both the impulsive and low-thrust case for a particular DRM, and the number of variations investigated, the “Create and Run Both” button provides one-click automation of the entire analysis.

### RESULTS

Table 1 shows the  $\Delta V$ s for all cases analyzed for a five year mission. The  $\Delta V$  is a function of the DRM characteristic since each DRM has a different number and sequence of stars observed in the same 5-year period. The use of the JWST orbit or the baseline orbit did not vary the resulting  $\Delta V$  much ( $\sim 2\%$ ) indicating that the selection of either a Class-I or a Class-II telescope orbit has little effect on the overall  $\Delta V$  budget. Note the difference in the  $\Delta V$  for each DRM. As the star selection was refined and the occulter diameter changed, a separation distance was selected for a given occulter diameter. The  $\Delta V$ s for DRM 2 and 3 used both 38,700 km and 72,000km while  $\Delta V$ s for DRM 4 and 5 were computed for only a specific occulter diameter. The  $\Delta V$  for a separation distance of 38,700 km averaged 3317 m/s for DRM 2 and were approximately 459 m/s ( $\sim 12\%$ ) less than the DRM 3 DV average of 3777 m/s. DRM 5 was the least expensive  $\Delta V$ . The change to a 72,000 km separation was used for comparison in DRM 2 and 3, but was required for DRM 4. These impulsive  $\Delta V$ s ranged from a low of 6058 m/s to 7180 m/s for a five year mission. The free space (no dynamics modeled) results shown in Table 1 are for comparison and is simply the summation of the calculations based on acceleration to represent the  $\Delta V$  to move a given distance for each observation.

Once a finite maneuver was implemented, only DRMs 4 and 5 were used as the other DRMs were considered not viable once these were generated. The finite maneuver

$\Delta V$  is approximately 15% higher than the impulsive  $\Delta V$  case. Remember that in both the impulsive and finite maneuver cases, the duration of the transfer time remains the same. Using the familiar rocket equation, the percentage fuel mass shown in Table 1 is based on an initial Occulter mass of 1000kg using a propulsion system with an Isp performance of 220 sec for impulsive and 4100 sec for finite – low thrust cases. This fuel mass was computed to show the relative mass allocation.

The  $\Delta V$  changes were determined to be mostly dependent upon the observation duration and when the star enters the field of regard of the telescope. The field of regard is based on sunlight infringement into the telescope itself along with spacecraft thermal requirements. Figures 17 and 18 show views of a complete 5-year mission from an oblique view and from along the Y-axis in a rotating coordinate system. While the oblique view gives an impression of a traditional (natural) Lissajous motion, the Y-axis view highlights the non-natural motion.

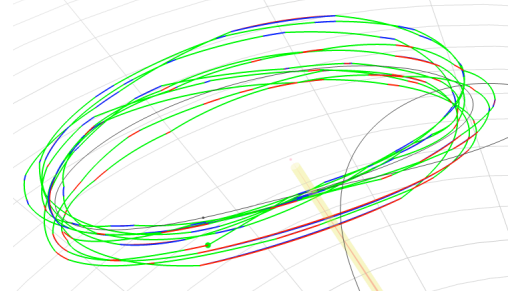


Figure 17: Oblique View of a Complete Mission in a Rotating System

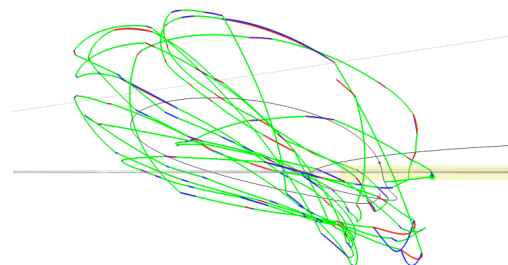


Figure 18: Y-Axis View of a Complete Mission in a Rotating System  
Individual  $\Delta V$ s range from a few m/s to 50 m/s with an average of 12 m/s for DRM-4

## IAC-08-C1.6.2

and 20 m/s for DRM-5. The magnitude depends upon the distance and duration of the transfer. These individual  $\Delta V$ s are shown in Figure 19 for DRM #4 and #5. Figure 20 presents the finite maneuver durations for DRM #5 which varies from 5 to 28 days. Also shown in this plot are the

durations of each observation which are on the order of 2 to 4 days. Note that no state or maneuver errors were introduced in this analysis, which could increase the  $\Delta V$  required.

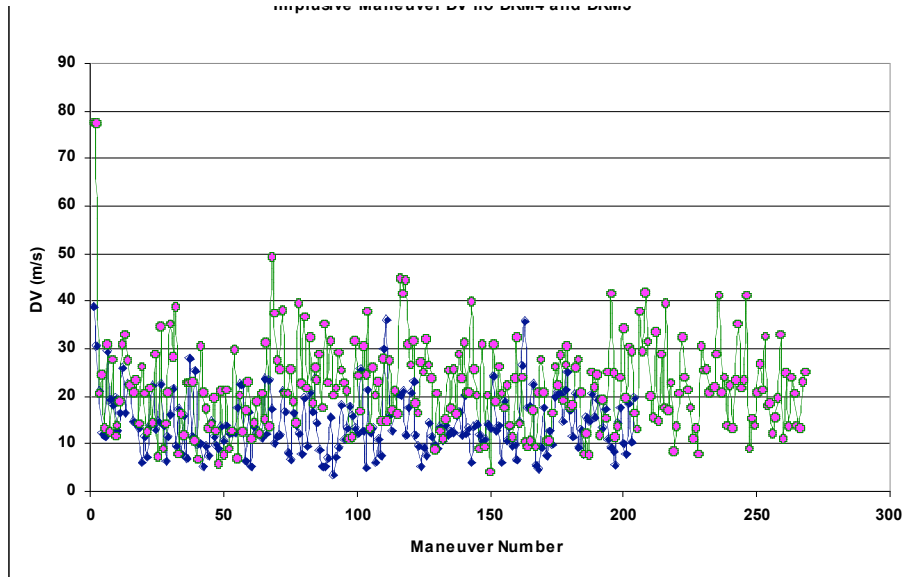


Figure 19: Individual  $\Delta V$ s for DRM #4 (blue) and #5 (green, longer duration)

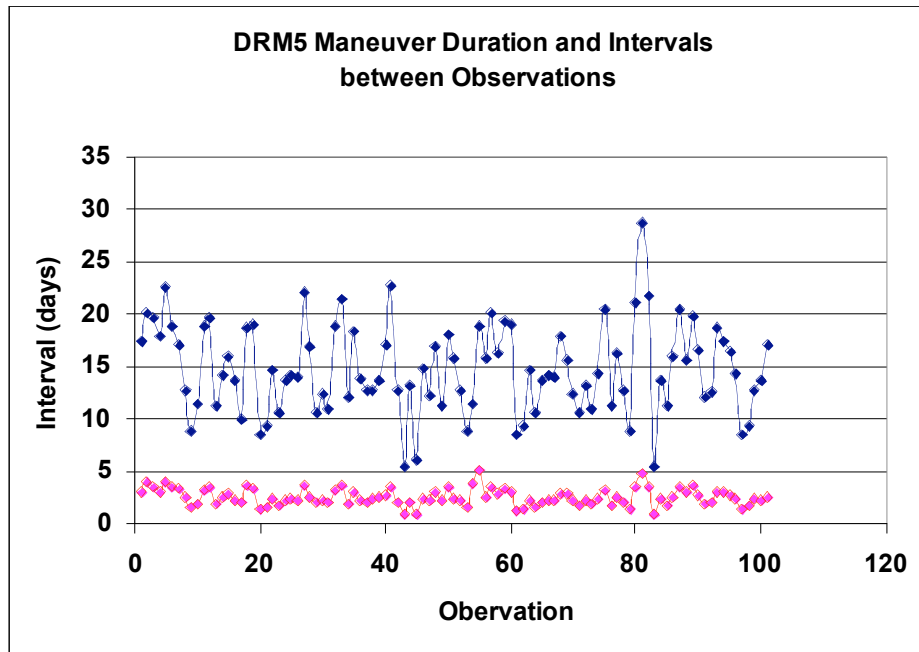


Figure 20: DRM # 4 and #5 Finite Maneuver Durations

## IAC-08-C1.6.2

### Comparison to Continuous Controllers Using Three-Body Dynamics for Accelerations

When the above results are compared to the continuous controllers described earlier, it was found that the  $\Delta V$  did not vary greatly. For example, when compared to Millard's LQR and NL Optimal Transits, the overall  $\Delta V$  difference are approximately 1% to 2% (comparing 5966 m/s and 6111 m/s to the 5904 m/s in this paper). In comparison to a simplified LQR using pseudopotential functions to determine the accelerations and a constant separation distance that follows a CRTB orbit, the  $\Delta V$  comparisons are on the order of 30%. As a final comparison, the impulsive implementation was changed to an optimization process for several maneuvers. The  $\Delta V$ s from this Astrogator optimization using a continuous control differed by only a few percent. The consistency between these results indicates that there may be a set of orbits and manifolds which minimize the fuel cost in this multiple gravitational field.

### CONCLUSIONS

This study shows that operation of the NWO formation design is feasible and poses no operational maneuver problems, given the propulsion systems modeled. Several DRMs were used which determine the star selection and separation distances. Results for each targeted maneuver in an entire mission, for both the impulsive and low-thrust cases, are readily available as well as mission-level summaries of total  $\Delta V$ , fuel used, and thrusting time required for the transfers. The DRM star sequence, the number of stars, and the separation distance all determine the required mission  $\Delta V$ . The impulsive  $\Delta V$ , while large compared to libration orbit maintenance strategies, is reasonable at a 3 km/s to 5 km/s range. Results for the low-thrust analyses show about a 15% increase in  $\Delta V$  over the impulsive cases while significantly decreasing the required fuel mass.

Table 1. Five-Year Mission  $\Delta V$  Results from DC Correction Method

Orbit Type JWST = Class-II Baseline = Class-I	DRM Applied (# 2 through #5)	Start of Simulation	38,700-km Impulsive $\Delta V$ (m/s)	72,000-km Impulsive $\Delta V$ (m/s)	72,000-km Finite (low- thrust) $\Delta V$ (m/s)	% of Total Mass Used for Fuel (assumes a 1000kg occultor)
JWST	2	Jan 2011	3236	---	---	78
JWST	3	Jan 2011	3695	---	---	82
Free Space	2	n/a	6122	---	---	94
Free Space	3	n/a	7010	---	---	96
Baseline	2	Jan 2011	3308	---	---	78
Baseline	2	April 2011	3398	6429	---	79 / 95
Baseline	2	May 2011	3367	6376	---	79 / 95
Baseline	2	Jan 2012	3198	6058	---	77 / 94
Baseline	3	Jan 2011	3781	6913	7587	83 / 82 / 17
Baseline	3	April 2011	3972	7182	7901	84 / 96 / 18
Baseline	3	May 2012	3726	7063	7790	82 / 96 / 18
Baseline	3	Jan 2012	3629	6877	7550	81 / 96 / 17
Baseline	4	April 2011	---	5904	7133	94 / 16
Baseline	5	April 2011	2951	---	3214	74 / 07

## IAC-08-C1.6.2

### REFERENCES

1. University of Colorado, Boulder, CO, <http://newworlds.colorado.edu/>
2. Webster Cash, "New Worlds Occulters" University of Colorado, September 29, 2006 New Worlds Occulters
3. Jonathan Arenberg, Northrop Grumman & Webster Cash, University of Colorado, *New Worlds Observer : A Novel Planet Finding Mission*, [http://www-luan.unice.fr/colloqueUAI/presentations/IAU/41\\_Jonathan\\_Arenberg.pdf](http://www-luan.unice.fr/colloqueUAI/presentations/IAU/41_Jonathan_Arenberg.pdf)
4. Detailed Reference Mission Study Notes from Dr. Don Lindler, GSFC NASA, 2007
5. M. Farrar, M. Thein, and D. Folta, "A Comparative Analysis Of Control Techniques For Formation Flying Spacecraft In An Earth/Moon-Sun L<sub>2</sub>-Centered Lissajous Orbit" AIAA/AAS Astrodynamics Specialist Conference, HI, 2008
6. L. Millard and K. Howell, "Optimal Reconfiguration Maneuvers for Spacecraft Imaging Arrays in Multi-Body Regimes", IAC-07-C1.7.03, 56th IAC, Hyderabad 24-28 September, 2007.
7. Marchand, B. "Spacecraft Formation Keeping Near the Libration Points of the Sun-Earth-Moon System", PhD Thesis, Purdue University, August 2004.
8. J. Masdemont, G. Gómez, M. Lo, and K. Museth, "Simulation of Formation Flight Near Lagrange Points for the TPF Mission," AAS/AIAA Astrodynamics Specialists Conference, Quebec, Canada. AAS Paper No. 01-305, Aug. 2001.
9. D. Folta, K. Hartman, K. Howell, B. Marchand, "Formation Control of the MAXIM L2 Libration Orbit Mission", AIAA/AAS Astrodynamics Specialist Conference, August 12-18, Providence Rhode Island.
10. J. Carrico, E. Fletcher, "Software Architecture and Use of Satellite Tool Kit's Astrogator Module for Libration Point Orbit Missions", Libration Point Orbits And Applications, Parador d'Aiguablava, Girona, Spain, June 2002
11. Analytical Graphics, Inc., 220 Valley Creek Blvd., Exton, PA 19341, USA, [info@agi.com](mailto:info@agi.com), [www.agi.com](http://www.agi.com)